



Automatic recognition system of pointer meters based on lightweight CNN and WSNs with on-sensor image processing

Liqun Hou^{*}, Huaisheng Qu

Department of Automation, North China Electric Power University, Baoding 071003, China

ARTICLE INFO

Keywords:
 Pointer Meter
 Reading Recognition
 Wireless Sensor Networks
 Convolutional Neural Network

ABSTRACT

The pointer meter is widely used in the modern industrial process. This paper proposes a novel pointer meter recognition method based on wireless sensor networks (WSNs) and a lightweight convolutional neural network (CNN), which completes image preprocessing, CNN classification, and reading calculation on the WSN end node, and then only transmits the recognized result in the WSN to reduce its payload transmission data. Meanwhile, a lightweight CNN classifier model with a simple structure and small size is designed for embedding in the resource-constrained WSN node. A set of experiments have been carried out on the fabricated prototype to verify the feasibility and adaptability of the proposed method. Experimental results have shown that the maximum error of the recognized results for real-world applications is around 0.27%, while the payload transmission data of the WSN decrease from 112.5 kB to 5 bytes.

1. Introduction

Although smart instruments have been widely employed in various application areas, a large number of pointer meters without computer interfaces are still used in modern industrial processes to monitor different devices and process parameters due to their inherent advantages such as low cost, high reliability, and simple structure. Generally, the readings of the pointer meter are manually obtained by the technician. This approach is time-consuming, inefficient, and inconvenient, especially in terrible weather conditions. Automatically inputting the readings to the existing monitoring systems, like Supervisory Control and Data Acquisition (SCADA), Advanced Metering Infrastructure (AMI), and Internet of Things (IoT), is helpful and significant for the system operator [1,2]. Automatically reading the pointer meter is also very useful for the temporary test needing to use the readings of the pointer meter because the installation of a new smart transducer would be inconvenient and require high cost.

Computer vision technology is a promising solution for the automatic recognition of the pointer meter. In the last two decades, researchers have explored various automated reading algorithms or systems for the pointer meter in various applications, like pointer meter automatic calibration [3,4], pointer meter automatic recognition [5–9], automobile dashboard detection [10]. Among these approaches, the angle method and the distance method are the two most popular methods. A

pointer meter automatic reading device using the angle method has been developed on an ARM platform in [5], while an automatic meter reading method for the meter with a non-uniform scale based on scale seeking and pointer distance method is proposed in [6]. Besides the basic reading recognition function, some enhanced algorithms are investigated by different researchers to address the possible interference during reading recognition in real-world applications. A real-time automatic recognition method is presented for the pointer meter under uneven illumination in [7], an inverse perspective mapping approach is used in [8] to correct the tilt of the pointer meter, and a binary threshold segmentation method is proposed in [9] to remove the influence of pointer shadows.

Recently, deep learning has achieved remarkable results in virtual recognition and speech recognition [11,12]. Some researchers have investigated using deep learning to recognize the pointer meter [13–16] as well. Liu et al. in [13] employed a faster region-based convolutional network (Faster RCNN) to detect the meter position, and then use the Hough transform and angle method to recognize meter reading. Lin et al. in [14] presented a meter recognition method based on an optimized single shot multibox detector (SSD) network. Zuo et al. in [15] proposed a robust meter reading recognition approach using improved mask-RCNN. Cai et al. in [16] introduced a virtual sample generation technology to obtain a large number of meter images from a small group of real meter images for the training of the meter recognition model based

* Corresponding author at: No.619, Yonghuabei Street Baoding 071003, China.

E-mail address: houliqun@ncepu.edu.cn (L. Hou).

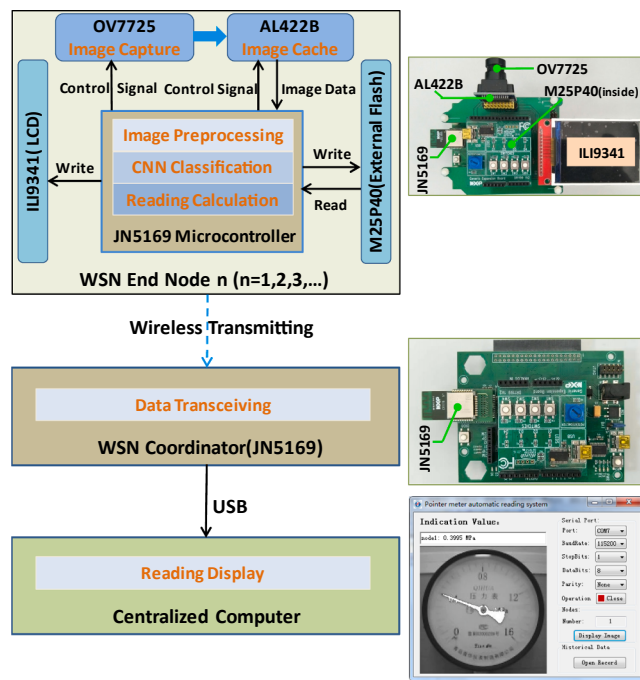


Fig. 1. Schematic diagram of the proposed system.

on CNN.

It can be seen that most of the pointer meter automatic recognition systems mentioned above are based on wired systems and PC [1,3,4,6–8,10,14–16] that requires additional cables and a large installation cost, while the systems introduced in [9,13] are designed to be used on expensive inspection robots.

Besides deep learning, wireless sensor network (WSN) is another research hot point in the last two decades. Currently, WSNs with cameras have been successfully applied in many image processing areas, such as vineyard monitoring [17] and hand gesture recognition [18]. Compared with a wired system, WSN has many inherent advantages like relatively low cost and convenient installation. Therefore, WSN is a potential low-cost and convenient solution for pointer meter automatic recognition. Our previous work in [19] explores the possibility of pointer meter recognition based on WSN using the traditional angle method. However, pointer meter recognition using WSNs and deep learning algorithm like CNN is a relatively unexplored field due to the tension between the high system requirement of image transmission and CNN classifier with the resource-constrained characteristics of WSNs nodes. Compared with the transmission of slow-changing scalar values such as temperature, image transmission needs a higher data transmission rate. Unfortunately, most of the current WSNs have limited radio bandwidths, which limit the wireless transmission of the image. Meanwhile, the limited computational and storage resource of the WSNs node often impedes the implementation of the complex pointer meter recognition algorithms like CNN classification on the node.

To address these tensions, a pointer meter recognition method based on WSNs and lightweight CNN is investigated, which achieves image preprocessing, CNN classification, and reading calculation on the WSN end node, and then only transmits the recognized reading in the WSN to reduce the payload transmission data. Meanwhile, a lightweight CNN classifier model with a simple structure and small parameter size is specifically designed for WSN applications. The proposed approach firstly determines the closest large scale to the pointer by the lightweight CNN classifier embedded on the WSNs node after off-line training and then calculates the inclination angle between the pointer and the large scale. Finally, the meter reading is obtained using the angle method based on the recognized large-scale value. The proposed method is

Table 1
Memory usage of the coordinator and the end node.

Application	Project template		Final program		Recognition algorithm	
	Flash/ kB	RAM/ kB	Flash/ kB	RAM/ kB	Flash/ kB	RAM/ kB
Coordinator	149.9	26.9	151.5	28.7	1.6	1.8
End node	143.2	23.9	189.8	28.7	46.6	4.8

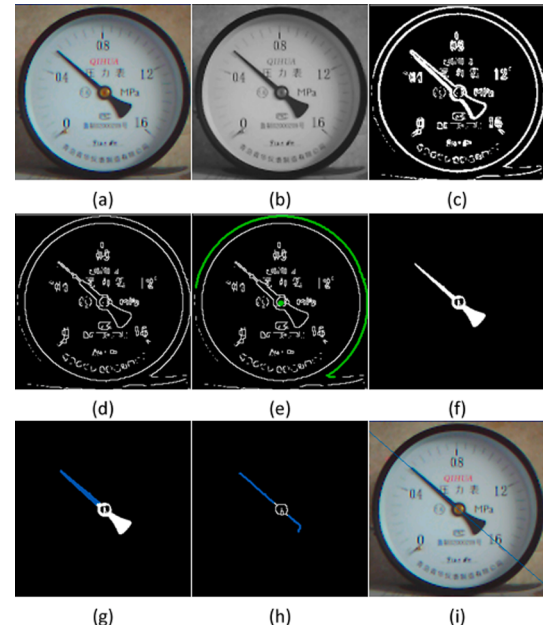


Fig. 2. Image processing procedure: (a) Original image, (b) Grayscale image, (c) Edge detection, (d) Image refinement, (e) Dial location, (f) Pointer extraction, (g) Pointer rod extraction, (h) Pointer refinement, (i) Pointer direction fitting.

verified on NXP JN5169 modules, a commercially available WSNs node with limited computational and storage resources.

The remainder of this article is organized as follows. The system architecture and implementation of the proposed system are described in Section II, while the experimental evaluation is given in Section III. Finally, Section IV presents the overall conclusion.

2. System architecture and implementation

The architecture of the proposed pointer meter recognition system based on a star topology WSN and CNN is sketched in Fig. 1. This star topology WSN based on ZigBee protocol consists of one coordinator and several end nodes. But for example purposes, only one end node is illustrated in detail in Fig. 1.

The proposed system completes image preprocessing, CNN classification, and reading calculation on the WSN end node, and then only transmits the recognized reading to the centralized computer through the WSN coordinator and USB interface. The image preprocessing procedure includes image graying, edge detection, edge refinement, round dial location, pointer detection, and pointer coordinates extraction. The extracted pointer coordinates are used as the input of the lightweight CNN classifier to determine the closest large scale to the pointer. In the reading calculation procedure, the inclination angle between the pointer and the large scale is calculated firstly, and the meter reading is then obtained using the angle method based on the large scale value.

This research selects JN5169, a high-performance wireless microcomputer from NXP, as the basic hardware platform of the WSN [20].

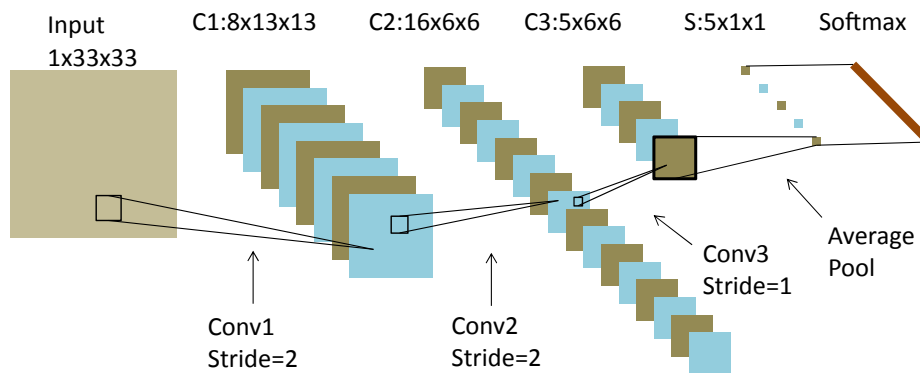


Fig. 3. The structure of the CNN.

Table 2
Parameter configuration of the CNN.

Network layer	Number of Filters	Size/Stride	Number of Bias	Outputs	Parameter Size	RAM Requirement
Conv1	8	9 × 9/2	8	8x13x13	2.56 kB	1.69 kB
Conv2	16	3 × 3/2	16	16x6x6	4.56 kB	3.83 kB
Conv3	5	1 × 1/1	5	5x6x6	0.33 kB	1.08 kB
Average pool	–	global	–	5x1x1	–	–

JN5169 supports IEEE 802.15.4 and ZigBee protocols and integrates a 32-bit RISC architecture with 512 kB Flash, 4 kB EEPROM, and 32 kB RAM. A 1/4-inch CMOS VGA image sensor chip, OV7725 manufactured by Omni Vision, is employed as the camera, while one 384 kB FIFO chip, AL422B from AverLogic, is used to buffer the image data from the OV7725. Finally, an external flash memory, M25P40 from STMicroelectronics, is used for image storage. An optional LCD is also designed for the convenience of system testing.

The application programs of the WSNs coordinator and end nodes are developed based on the project template provided by NXP. The project template provides the basic functions of a ZigBee protocol. The memory used by the project template, final program, and the proposed pointer meter recognition algorithm is given in Table 1. It can be seen that 151.5 kB Flash and 28.7 kB RAM are needed for the final program on the WSNs coordinator, while 189.8 kB Flash and 28.7 kB RAM are used by the final program of the end node.

2.1. Image preprocessing

The output of the image sensor (OV7725) is a 240*240 pixels image in RGB565 format. The original image of a pointer meter is shown in Fig. 2(a). The size of the image reduces from 115,200 bytes to 57,600 bytes by graying. The grayscale image, as shown in Fig. 2(b), is stored in the external flash (M25P40). Sobel edge detection is then used to obtain the edges of the meter image, as shown in Fig. 2(c). After edge detection, Zhang-Suen thinning algorithm is adopted to refine the image. The refined skeleton of the image in one pixel width is shown in Fig. 2(d). The Eight-neighbor method is then used to find the meter boundary. After finding the meter boundary, the improved Hough transform for circle detection proposed in [21] is used to obtain the center coordinate of the dial. The boundary and center of the dial are shown in Fig. 2(e) in green color. The regional growth method is then used to extract the pointer, during which the Otsu algorithm is employed to obtain the threshold while the pixel around the center with the smallest grayscale is used as the growing seed. The extracted pointer is shown in Fig. 2(f).

2.2. CNN classification

The extracted pointer coordinates in image preprocessing are then re-arrayed and input into CNN to determine the closest large scale to the

pointer. This research uses a memory-optimized CNN structure based on the CNN structure proposed in [22], which removes the fully connected layer to reduce the number of CNN parameters. The used network structure is shown in Fig. 3, while the size of network parameters is given in Table 2.

This CNN consists of one input layer, three convolutional layers, one average pooling layer, and one softmax layer. Its total parameter size is about 7.45 kB, which is far below the flash size (512 kB) of JN5169. The largest RAM requirement of the convolutional layers is about 3.83 kB, which is small than the size of the RAM provided by JN5169 for the user's application program (5 kB).

In this research, only the coordinate of the pointer rod is used as the input of the CNN because we find that the classification accuracy of the CNN only using the pointer rod coordinates as the input is higher than the CNN using the entire pointer coordinates. Based on the image in Fig. 2(f), the pointer rod is extracted and shown in Fig. 2(g) in blue color. As the CNN input usually is two-dimensional data and the maximum pixel number of the pointer rod is around 338, the extracted pointer rod coordinates are re-arrayed to a 26*26 array, and then extended to a 33*33 array by filling zeros. Finally, the extended 33*33 array is used as the actual input of the CNN.

The CNN used in this research includes three convolutional layers (Conv1, Conv2, Conv3), and each convolutional layer is followed by a rectified linear unit (ReLU). Unlike traditional CNN structure, no pooling layer is inserted between two adjacent convolutional layers, and the strides of Conv1, Conv2, and Conv3 are 2, 2, 1, respectively. This structure significantly reduces the complexity of the CNN and has similar classification effectiveness as the CNN with the pooling layer. Following Conv3, an average pooling layer is used to calculate the average value of the Conv3 outputs.

The average pooling layer outputs are sent to the softmax function. The output of the softmax function is an $n \times 1$ vector that represents the matching probability for each large-scale value of the meter. In this research, $n = 5$. The output with maximum probability is the closest large scale to the pointer.

2.3. Reading calculation

The extracted pointer by image preprocessing is refined and filtered to remove the interference pixels around the meter center, as shown in



Fig. 4. The principle diagram of meter reading calculation.

Fig. 2(h). The improved Hough transform algorithm for line detection proposed in [23] is then used to fit the line where the meter pointer is located. The obtained fit line is shown in Fig. 2(i). Finally, the angle method based on the large scales is employed to obtain the meter reading (P). The principle of the reading calculation is shown in Fig. 4, and the following equation is used to calculate the reading:

$$P = P_{ls_CNN} \pm \frac{|\theta - \theta_{ls}|}{\theta_i} * P_i \quad (1)$$

where P_{ls_CNN} is the large scale determined by CNN classifier, θ is the inclination angle of the pointer, θ_{ls} is the angle between the large scale and the horizontal line, θ_i is the angle between two adjacent large scales. In this case, P_{ls_CNN} is 0.4 MPa, P_i is 0.4 MPa (0.8–0.4 MPa), θ , θ_{ls} , and θ_i , are 41.79°, 20.33°, 67.82°, respectively, the obtained meter reading is 0.53 MPa.

3. Experimental validation

A series of experiments are conducted on various pointer meters to verify the feasibility of the presented system and its adaptability to different working environments. In this paper, single-pointer pressure meters and the related calibration devices are used as an example.

3.1. Experimental setup

The experimental setup is shown in Fig. 5. The four WSN end nodes are installed directly facing the pointer meters through adjustable brackets, while the WSN coordinator is connected with a laptop via USB. The pressure value can be modulated by rotating the handle.

3.2. CNN classifier training and testing

The CNN classifier is trained to determine the closest large scale to the pointer. As shown in Fig. 6, the pressure meter used in this

experiment has five large scales, namely a, b, c, d, and e in Fig. 6(f), corresponding to 0, 0.4, 0.8, 1.2, and 1.6 MPa. When the pointer locates in the middle of two large scales, either large scale can be used as the closest one.

The CNN classifier model is built and trained in MATLAB. The learning rate, minimum batch size, and momentum coefficient for training the CNN model are selected through a repeated testing and comparing process. Finally, 0.01, 20, and 0.95 are used for the learning rate, minimum batch size, and momentum coefficient, due to the best training results they have. The training procedure is completed on a PC with a 2.5 GHz CPU and 8 GB RAM. 600 sets of images under strong, normal, and less illumination, 120 sets for every large scale, are collected to train the CNN classifier, while 800 sets of images are employed to test the classifier. The training data only use the images whose reading is close to the large scale, while the test data employ the images with various readings in the whole measurement range. Therefore, the training dataset is smaller than the testing dataset. The testing results of the CNN classifier model are given in Table 3. It can be seen that the classification accuracy reaches 100%. In this paper, the CNN classifier is only used to determine the closest large scale to the pointer, and when the pointer is in the middle of two large scales, either large scale can be used as the right one. Thus, the learning capability of the CNN classifier is sufficient for this application, and the classification

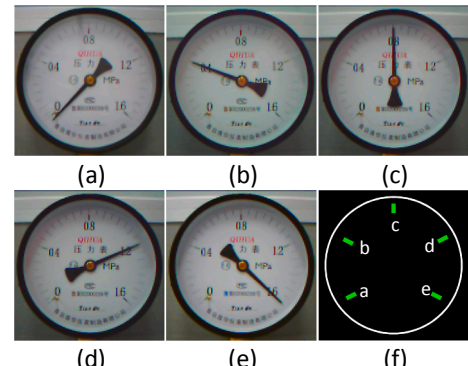


Fig. 6. The large scales of the meter.

Table 3
The training and testing results of the CNN classifier.

Training data set	Testing data set	Classification Accuracy
600	800	100%

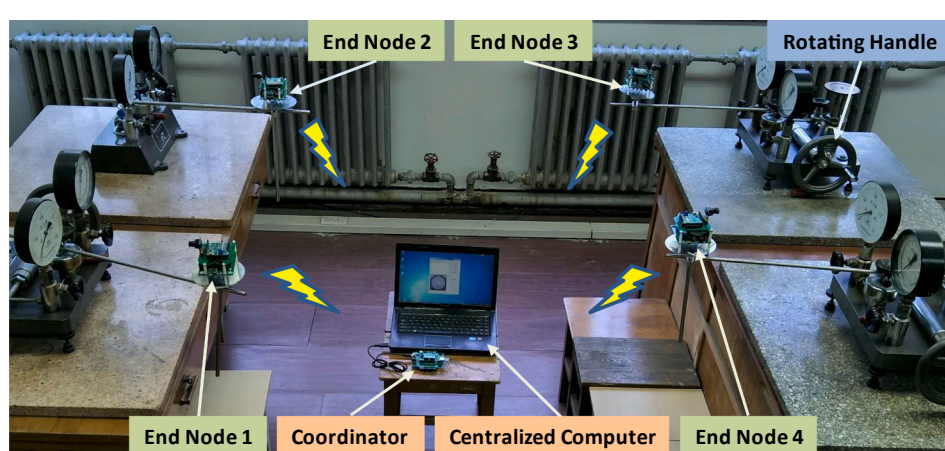


Fig. 5. View of the experimental setup.

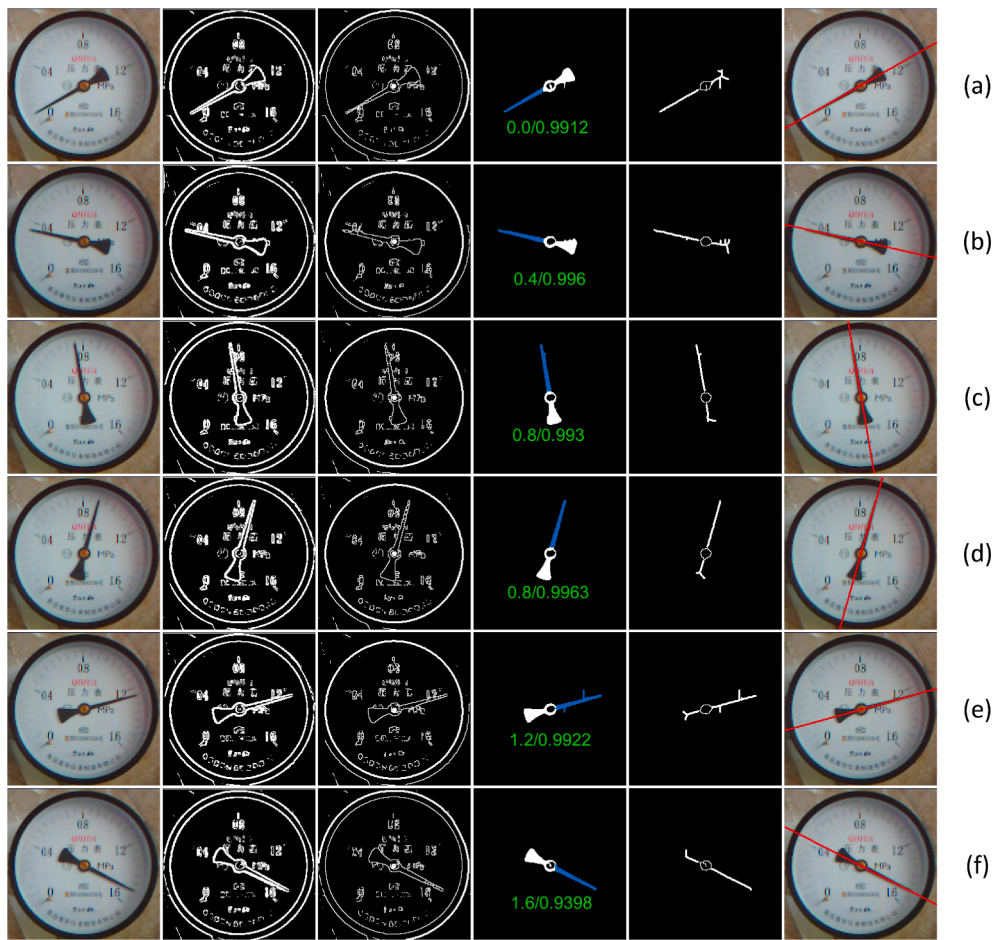


Fig. 7. The experimental results of the meter with various readings.

Table 4

The recognition errors of the meter with various readings.

Num	Actual values/MPa	System recognition results			Absolute error/MPa	Fiducial error/%
		CNN classifier outputs /Matching rate	Deviation values/MPa	recognized results/MPa		
1	0.1	0.0/0.9912	+0.0990	0.0990	-0.0010	-0.06
2	0.15	0.0/0.9181	+0.1516	0.1516	0.0016	0.10
3	0.35	0.4/0.9960	-0.0501	0.3499	-0.0001	-0.01
4	0.5	0.4/0.9838	+0.0994	0.4994	-0.0006	-0.04
5	0.75	0.8/0.9930	-0.0497	0.7503	0.0003	0.02
6	0.9	0.8/0.9963	+0.1022	0.9022	0.0022	0.14
7	1.05	0.8/0.5133	+0.2497	1.0497	-0.0003	-0.02
8	1.25	1.2/0.9922	+0.0495	1.2495	-0.0005	-0.03
9	1.4	1.2/0.6333	+0.2001	1.4001	0.0001	0.01
10	1.5	1.6/0.9398	-0.0988	1.5012	0.0012	0.08

accuracy of the proposed method reaches 100%. After the CNN classifier model is well trained, it is embedded in the WSN end nodes.

3.3. Pointer meter recognition

To verify the feasibility of the proposed method, the meter with various readings is recognized in the laboratory with ideal working environments. As shown in Fig. 7, the original meter image and the obtained results in the recognition process, namely the results of edge detection, dial location, pointer rod extraction, pointer refinement, and pointer direction fitting, are given in sequence from the first to the sixth column. The green numbers in the fourth column in Fig. 7 indicate the recognized large scale by the CNN classifier and its matching rate.

More detailed experimental data are given in Table 4. The CNN

classifier outputs and the matching rate are the recognized large scale by the CNN classifier and its matching rate. The deviation values mean the deviation between the pointer and the closest large scale. The sum of CNN classifier output and the deviation value will be the final recognized value of the meter. It is clear that the maximum absolute error is 0.0022 MPa, while the maximum fiducial error is 0.14%. Compared with the accuracy (1.6%) of the pressure meter used in this test, this error level is acceptable.

3.4. Recognition of meters with blur, dirty points, and less illumination

To evaluate the robustness of the proposed meter recognition approach for real-world applications, we test its recognition accuracy for the meters with blur, dirty marks, and less illumination. The meter

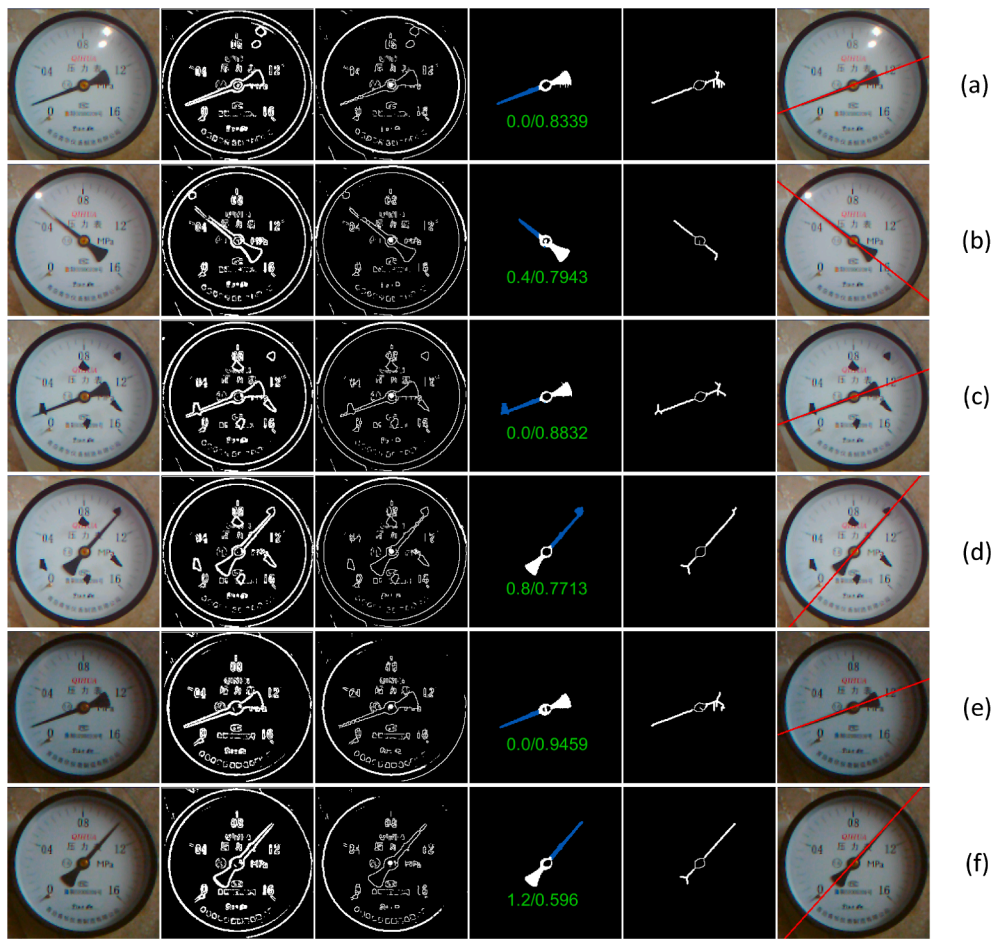


Fig. 8. The experimental results of the meters with blur, dirty marks, and less illumination.

Table 5

The recognition errors of the meters with blur, dirty marks, and less illumination.

Group	Num	Actual values/ MPa	System recognition results			Absolute error/ MPa	Fiducial error/ %
			CNN classifier outputs /Matching rate	Deviation values/ MPa	Recognized results/ MPa		
Blur	1	0.15	0.0/0.8339	+0.1501	0.1501	0.0001	0.01
	2	0.5	0.4/0.7943	+0.1019	0.5019	0.0019	0.12
	3	1.05	0.8/0.8885	+0.2539	1.0539	0.0039	0.24
	4	1.5	1.6/0.9711	-0.0980	1.5020	0.0020	0.13
Dirty mark	1	0.15	0.0/0.8832	+0.1533	0.1533	0.0033	0.21
	2	0.5	0.4/0.9814	+0.1028	0.5028	0.0028	0.18
	3	1.05	0.8/0.7713	+0.2460	1.0460	-0.0040	-0.25
	4	1.5	1.6/0.9593	-0.0979	1.5021	0.0021	0.13
Less illumination	1	0.15	0.0/0.9459	+0.1530	0.1530	0.0030	0.19
	2	0.5	0.4/0.9915	+0.1043	0.5043	0.0043	0.27
	3	1.05	1.2/0.5960	-0.1538	1.0462	-0.0038	-0.24
	4	1.5	1.6/0.9492	-0.0972	1.5028	0.0028	0.18

recognition process is shown in Fig. 8, while more detailed experimental results are given in Table 5.

We can see from Table 5 that the maximum absolute errors for the meters with blurs, dirty marks, and less illumination are 0.0039, -0.0040, and 0.0043 MPa, while the maximum fiducial errors are 0.24%, -0.25%, and 0.27%, respectively. Although the maximum fiducial error increases from 0.14% to 0.27%, it is still acceptable for the accuracy (1.6%) of the pressure meter used in this experiment.

3.5. Recognition of various meters

To evaluate the adaptability of the proposed method to various meters, two different pressure meters with similar measurement ranges and large-scale distribution as the one used in the last section are tested in this experiment. The meter recognition process is shown in Fig. 9, while more detailed experimental results are given in Table 6.

It can be seen from Table 6 that the maximum absolute errors of the two meters are -0.0021 and -0.0039 MPa, while the maximum fiducial errors are -0.13% and -0.24%.

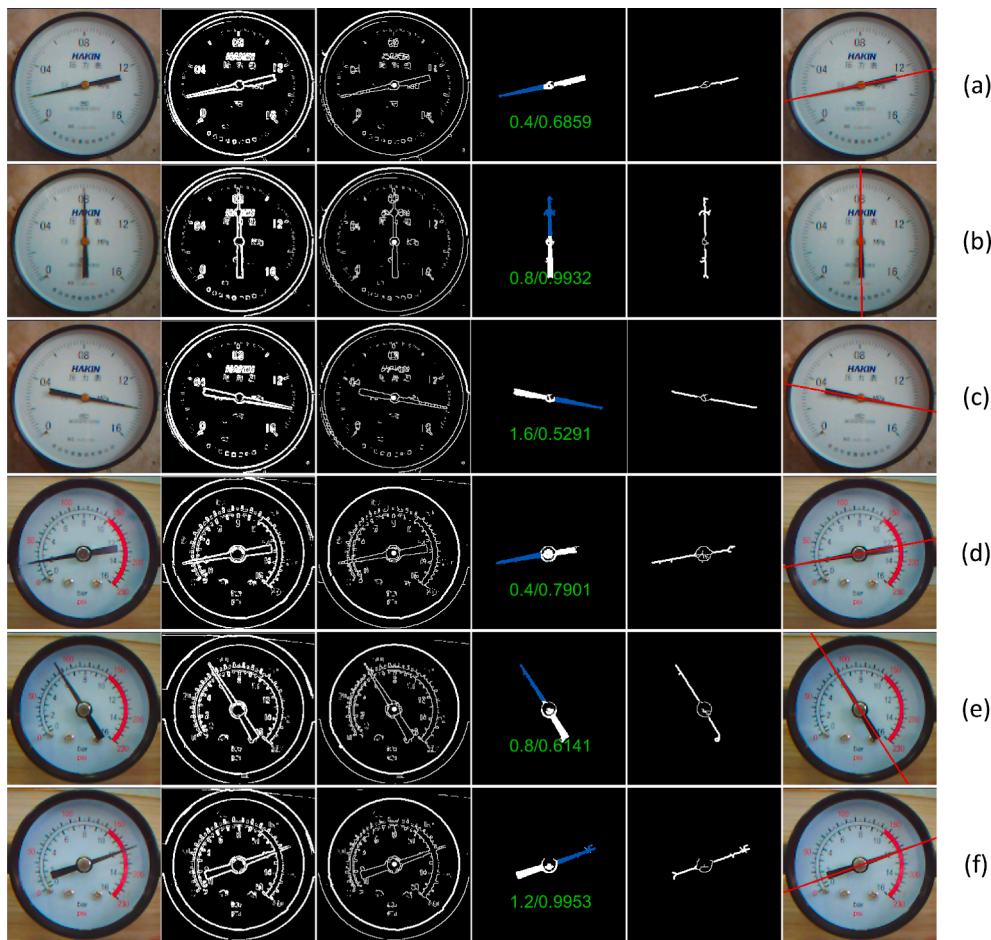


Fig. 9. The experimental results of two different meters with various readings.

Table 6

The recognition errors of two different meters with various readings.

Group	Num	Actual values/MPa	System recognition results			Absolute error/MPa	Fiducial error/%
			CNN classifier outputs /Matching ratio	Deviation values/ MPa	Recognized results/ MPa		
Meter 1	1	0.2	0.4/0.6859	-0.2021	0.1979	-0.0021	-0.13
	2	0.5	0.4/0.9455	+0.0994	0.4994	-0.0006	-0.04
	3	0.8	0.8/0.9932	+0.0013	0.8013	0.0013	0.08
	4	1.0	0.8/0.8486	+0.2012	1.0012	0.0012	0.08
	5	1.4	1.6/0.5291	-0.2012	1.3988	-0.0012	-0.08
Meter 2	1	0.1	0.0/0.9068	+0.0996	0.0996	-0.0004	-0.03
	2	0.2	0.4/0.7901	-0.2039	0.1961	-0.0039	-0.24
	3	0.6	0.8/0.6141	-0.2010	0.5990	-0.0010	-0.06
	4	0.95	0.8/0.9109	+0.1531	0.9531	0.0031	0.19
	5	1.2	1.2/0.9953	+0.0021	1.2021	0.0021	0.13

3.6. Comparison of angle method and the proposed method

The scale distribution of a pointer meter is usually non-uniform. This will cause the accumulation of the recognition error of the angle method. To reduce this error accumulation, this paper uses a CNN classifier to determine the large-scale value of the pointer meter, and then calculate the reading value using the angle method based on the recognized large-scale value. The accuracy comparison of the proposed method and angle method is given in Table 7. It can be seen that the average error of our method is 0.0014 Mpa, which is significantly smaller than the average error of the angle method (0.0069 Mpa).

4. Conclusion

In this paper, we proposed a novel pointer meter recognition method based on WSN and CNN, which firstly determined the closest large scale to the pointer by the CNN classifier embedded on the WSNs node, and then obtained meter reading by combining the large scale and the inclination angle between the large scale and the pointer. To address the tension between the high data transmission rate of image transmission and the limited radio bandwidth of WSNs, the proposed system completed image preprocessing, CNN classification, and reading calculation on the WSN end node, and only transmitted the recognized reading to the centralized computer through the WSN. To reduce the requirement of computational and storage ability of the hardware

Table 7

The comparison of the angle method and the proposed method.

Num	Actual values/ MPa	Angle method		The proposed method	
		Reading/ MPa	Absolute error/MPa	Reading/ MPa	Absolute error/MPa
1	0.1	0.0891	-0.0109	0.0960	0.0040
2	0.2	0.1910	-0.0090	0.1965	-0.0035
3	0.4	0.3905	-0.0095	0.4017	0.0017
4	0.5	0.4887	-0.0113	0.4987	-0.0013
5	0.6	0.5906	-0.0094	0.5994	-0.0006
6	0.7	0.6931	-0.0069	0.7008	0.0008
7	0.8	0.7949	-0.0051	0.8013	0.0013
8	0.9	0.8941	0.0059	0.8997	-0.0003
9	1.0	0.9962	0.0038	1.0008	0.0008
10	1.2	1.1977	-0.0023	1.2005	0.0005
11	1.4	1.3979	-0.0021	1.3993	-0.0007
Average error/ Mpa		0.0069		0.0014	

platform, a lightweight CNN classifier model was adopted in this approach. A set of experiments have been conducted on the prototype to evaluate the feasibility and adaptability of the proposed method. Experimental results have shown that the maximum fiducial error of the recognized results for real-world applications was around 0.27%. Moreover, the proposed approach could significantly reduce the payload transmission data of the WSN from 112.5 kB to 5 bytes.

CRediT authorship contribution statement

Liqun Hou: Conceptualization, Methodology, Writing - original draft, Writing - review & editing, Supervision. **Huaisheng Qu:** Software, Validation, Investigation, Writing - original draft.

Declaration of Competing Interest

The authors declare that they have no known competing financial interests or personal relationships that could have appeared to influence the work reported in this paper.

Acknowledgments

This research was supported by the Natural Science Foundation of Hebei Province, China (Grant No. F2016502104).

References

- [1] C. Zheng, S. Wang, Y. Zhang, P. Zhang, Y. Zhao, A robust and automatic recognition system of analog instruments in power system by using computer vision, Measurement 92 (2016) 413–420.
- [2] Y. Tang, C. Ten, C. Wang, G. Parker, Extraction of energy information from analog meters using image processing, IEEE Trans. Smart Grid 6 (2015) 2032–2040.
- [3] F. Correa Alegria, A. Cruz Serra, Automatic calibration of analog and digital measuring instruments using computer vision, IEEE Trans. Instrum. Meas. 49 (2000) 94–99.
- [4] P.A. Belan, S.A. Araujo, A.F.H. Librantz, Segmentation-free approaches of computer vision for automatic calibration of digital and analog instruments, Measurement 46 (2013) 177–184.
- [5] Y. Cui, W. Luo, Q. Fan, Q. Peng, Y. Cai, Y. Yao, C. Xu, Design and implementation of pointer-type multi meters intelligent recognition device based on ARM platform, J. Phys. Conf. Ser. (2018).
- [6] H. Lai, Q. Kang, L. Pan, and C. Cui, “A novel scale recognition method for pointer meters adapted to different types and shapes,” in 15th IEEE International Conference on Automation Science and Engineering (IEEE CASE), Vancouver, BC, Canada, 2019, pp. 374–379.
- [7] Y. Rao, F. Yan, Y. Zhuang, and G. He, “A real-time auto-recognition method for pointer-meter under uneven illumination,” in 2019 IEEE International Conference on Real-Time Computing and Robotics, Irkutsk, Russia, 2019, pp. 890–894.
- [8] H. Bao, Q. Tan, S. Liu, and J. Miao, “Computer vision measurement of pointer meter readings based on inverse perspective mapping,” APPLIED SCIENCES-BASEL, vol. 9, 2019.
- [9] M. Yifan, J. Qi, A robust and high-precision automatic reading algorithm of pointer meters based on machine vision, Meas. Sci. Technol. 30 (2019), 015401.
- [10] H. Gao, M. Yi, J. Yu, J. Li, X. Yu, Character segmentation-based coarse-fine approach for automobile dashboard detection, IEEE Trans. Ind. Inf. 15 (2019) 5413–5424.
- [11] K. He, X. Zhang, S. Ren, J. Sun, Spatial pyramid pooling in deep convolutional networks for visual recognition, IEEE Trans. Pattern Anal. Mach. Intell. 37 (2015) 1904–1916.
- [12] O. Abdel-Hamid, A. Mohamed, H. Jiang, L. Deng, G. Penn, D. Yu, Convolutional neural networks for speech recognition, IEEE Trans. Audio Speech Lang. Process. 22 (2014) 1533–1545.
- [13] Y. Liu, J. Liu, Y. Ke, A detection and recognition system of pointer meters in substations based on computer vision, Measurement 152 (2020).
- [14] L. Lin and Z. Lu, “A pointer meter detection method based on optimal SSD network,” in 2019 IEEE 4th Advanced Information Technology, Electronic and Automation Control Conference (IAEAC), Piscataway, NJ, USA, 2019, pp. 1670–4.
- [15] L. Zuo, P. He, C. Zhang, Z. Zhang, A robust approach to reading recognition of pointer meters based on improved mask-RCNN, Neurocomputing 388 (2020) 90–101.
- [16] W. Cai, B. Ma, L. Zhang, Y. Han, A pointer meter recognition method based on virtual sample generation technology, Measurement 163 (2020).
- [17] J. Lloret, I. Bosch, S. Sendra, A. Serrano, A wireless sensor network for vineyard monitoring that uses image processing, Sensors 11 (2011–01–01 2011) 6165–6196.
- [18] T. Ganokratanaa, S. Pumrin, Hand gesture recognition algorithm for smart cities based on wireless Sensor, Int. J. Online Eng. 13 (2017) 58–75.
- [19] L. Hou and Q. Zhang, “Wireless sensor networks for pointer meter recognition,” in International Conference on Communication Technology Proceedings, ICCT, 2019, pp. 978–981.
- [20] “Data Sheet: JN516x IEEE802.15.4 Wireless Microcontroller, [Access Dec. 2020]. [Online]. Available: <https://www.nxp.com.cn/docs/en/data-sheet/JN516X.pdf>”.
- [21] X. Chen, Q. Wang, B. Li, Improved Hough algorithm for circle detection, Chinese J. Comput. Syst. Appl. 24 (2015) 197–201.
- [22] D. Han and H. Kim, “A number recognition system with memory optimized convolutional neural network for smart metering devices,” in 17th International Conference on Electronics, Information and Communication, Honolulu, HI, United states, 2018, pp. 1–4.
- [23] D. Ruijiao, Z. Wei, H. Songling, C. Jianye, Fast line detection algorithm based on improved Hough transformation, Chinese J. Sci. Instr. 31 (2010) 2774–2780.